

## Disorder-induced vibration-mode coupling in SiO<sub>2</sub> films observed under normal-incidence infrared radiation

I. Montero, L. Galán, O. Najmi, and J. M. Albella

*Instituto de Ciencia de Materiales, Consejo Superior de Investigaciones Científicas, and Departamento de Física Aplicada, Universidad Autónoma, C-XII Cantoblanco, 28049 Madrid, Spain*

(Received 22 February 1993; revised manuscript received 26 April 1994)

We have investigated the strongest infrared absorption mode in silicon oxide films obtained at low temperatures (anodic and plasma oxides). The asymmetric stretching transverse mode of the Si-O<sub>4</sub> tetrahedra, centered at 1070 cm<sup>-1</sup>, exhibits an interesting multiple-resonance structure on the high-energy side of the infrared spectrum. A transverse-optical (TO) mode at 1200 cm<sup>-1</sup> and a longitudinal-optical (LO) mode at 1150 cm<sup>-1</sup>, both modes associated with a LO-TO frequency splitting, and another longitudinal-optical mode at 1250 cm<sup>-1</sup>, associated also with a LO-TO splitting of the 1250- and 1070-cm<sup>-1</sup> peaks are also observed. An important increase in the intensity of the multiple-resonance feature, attributed to the water concentration present during the oxidation process, is observed. This effect is related to the increase in the short-range disorder in silicon oxide films attributed to OH and H<sub>2</sub>O incorporation during growth. In addition, x-ray-photoelectron-spectroscopy measurements reflect the influence of this short-range disorder on the O 1s and Si 2p core-level and valence-band spectra.

Because of the good physicochemical properties of the SiO<sub>2</sub> film, the understanding of its structure has represented one of the basic challenges of recent decades. SiO<sub>2</sub> films are generally noncrystalline. However, this is not necessarily associated with a complete lack of ordering.<sup>1,2</sup> Thus, the infrared optical properties of silica glass are close to those of crystalline SiO<sub>2</sub> in ring-shaped structures. In both cases, the Si-O<sub>4</sub> tetrahedra are held together via a bridging oxygen atom. In the amorphous state, the resulting distribution of the tetrahedra in ring-shaped structures with different sizes is made possible, to a large extent, by the flexibility of the Si-O-Si bond angle subtended by the bridging oxygen.<sup>2</sup>

Three well-known transverse-optical modes of the Si-O-Si group, identified as asymmetric, TO<sub>1</sub> (at ~1070 cm<sup>-1</sup>), rocking, TO<sub>rock</sub> (at ~460 cm<sup>-1</sup>), and bending, TO<sub>bend</sub> (at ~800 cm<sup>-1</sup>), were reported earlier in transmission ir measurements in silicon oxides. The absorption strength in each band rises linearly with the amount of oxygen in the films.<sup>3</sup> However, the TO<sub>rock</sub> mode of the Si-O<sub>4</sub> tetrahedra, in which the oxygen motion is out of the Si-O-Si plane, and the TO<sub>bend</sub> mode, in which the oxygen motion is in the plane and along the bisector of the Si-O-Si angle (~150°), were observed to be almost insensitive to structure changes.<sup>4</sup>

On the other hand, the TO<sub>1</sub> mode, in which the oxygen atom motion is in the Si-O-Si plane and parallel to the Si-Si line, shows the strongest ir absorption in silicon oxides, and the intensity depends on the magnitude of the dipole moment transition. However, it is important to realize that the situation is rarely so simple as to have an absorption band entirely caused by an isolated motion such as bond stretching. The long-ranged interactions between the tetrahedra, provided by the Coulomb fields, are necessary to explain the complete spectra.<sup>5</sup> In any case, the infrared absorption intensities of TO<sub>1</sub> modes

have been shown to obey Lambert-Bouguer's law within experimental errors.<sup>6,7</sup>

In this study we have chosen the prominent TO<sub>1</sub> peak as the most representative and sensitive to structural changes of the silicon oxide films. The intensity, position, and profile of the band are dependent on the oxygen-to-silicon atomic ratio, and vary with the formation conditions of the film. Peak shifts in the infrared absorption and chemical shifts in the x-ray photoelectron (XPS) spectra of different oxide phases have been consistently explained as changes in the oxidation state.<sup>8,9</sup> In this regard, the presence of water during the oxidation of silicon (at low and high temperatures) may produce important variations in the kinetics of formation and also in the properties of the silicon oxide films. For instance, in the case of silicon oxides obtained by room-temperature anodic oxidation, we have observed previously a transition from compact oxide to porous oxide when the water concentration in the electrolyte increases.<sup>10</sup>

High-purity (111) float-zone (FZ) silicon plates (oxygen content <10<sup>17</sup> at./cm<sup>2</sup>) with thickness of 350 μm were used as substrates for the ir study of the SiO<sub>2</sub> films. Thus, the absorption band at 1104 cm<sup>-1</sup>, which appears in the ir spectra due to the interstitial oxygen in the silicon substrate, disturbing the shape of the main absorbance structure at ~1070 cm<sup>-1</sup>, is not detected. The SiO<sub>2</sub> films were grown by low-temperature anodic oxidation under galvanostatic conditions, the electric current density being 5.00 mA cm<sup>-2</sup>. The electrolyte was KNO<sub>3</sub> dissolved in ethylene glycol at different water concentrations C<sub>w</sub> (see Table I). Thermal and plasma oxidation were also used for comparison. Other details on sample preparation are given elsewhere.<sup>11</sup>

All ir absorption measurements were carried out using a double beam spectrophotometer (Hitachi 270-50). Each spectrum is the average data accumulated from ten suc-

TABLE I. FWHM of XPS Si 2*p* and O 1*s* core levels of silicon oxide obtained at different experimental conditions. The value for Si is given as a resolution reference.

Treatments	Temperature (°C)	FWHM (eV)	
		Si 2 <i>p</i>	O 1 <i>s</i>
Thermal oxide	1200	1.45	1.50
$C_w=0\%,0.020M$	20	1.55	1.55
$C_w=0\%,0.019M$	20	1.60	1.80
$C_w=50\%,0.020M$	20	1.60	1.80
$C_w=100\%,0.020M$	20	1.65	1.85
Plasma oxide	950	1.85	1.95
Native oxide	~20	2.35	2.70
Si (single crystal)		1.20	

cessive scans. The spectra were run in the frequency regime from 4000 to 400  $\text{cm}^{-1}$  at room temperature. The spectral resolution was set at 2  $\text{cm}^{-1}$ . XPS measurements were also made on the  $\text{SiO}_2$  films using VGS ESCALAB 210 equipment with a Mg  $K\alpha$  x-radiation source and 0.3-eV analyzer resolution. These measurements have also been described in another work.<sup>11</sup>

Previous papers have shown that the  $\text{TO}_1$  mode (adjacent oxygen atoms move in phase) exhibits a multiple-resonance structure of the main Si-O stretching vibration, showing a shoulder on the high-frequency side.<sup>12-14</sup> This shoulder has usually been observed on thin silicon oxide films, under oblique incidence angle with unpolarized light.<sup>15</sup> Longitudinal optical (LO) modes are observed as well in addition to transverse-optical (TO) modes.<sup>16</sup> In this work, from ir measurements performed under normal incidence in the transmission mode, the multiple resonance of the  $\text{TO}_1$  mode has been observed for thick silicon oxides (> 30 nm). Curve-fitting procedures permit us to obtain the strength of this band. We have deconvoluted the multiple structure on the high-energy side of the  $\text{TO}_1$  peak in the 1100–1300  $\text{cm}^{-1}$  region into several Gaussian-broadened Lorentzian profiles. We tried a deconvolution into only three symmetrical Gaussian-Lorentzian contributions by a least-squares procedure: (i) the asymmetric stretching  $\text{TO}_2$  mode at approximately 1200  $\text{cm}^{-1}$ , in which the oxygen atoms move out of phase, (ii) the disorder-induced  $\text{LO}_2$  mode at ~1150  $\text{cm}^{-1}$ , and (iii) the peak located at ~1250  $\text{cm}^{-1}$ , which has been reported as a longitudinal-optical ( $\text{LO}_1$ ) resonance mode.<sup>17-19</sup> Finally, the main  $\text{TO}_1$  mode is also fitted into only one symmetrical Gaussian-Lorentzian contribution, with intensity  $I_m$ . Thus, the energies of the different contributions as well as the corresponding absorption band strengths have been accurately determined.

The resulting  $\text{LO}_2$ - $\text{TO}_2$  pair could be explained by assuming coupling effects associated with the network disorder, although the long-range Coulomb forces may also produce LO-TO splitting of the strongest infrared-active modes.<sup>2,17-21</sup> The  $\text{LO}_1$  mode (1250  $\text{cm}^{-1}$ ) is normally infrared inactive. However, it becomes infrared active, for instance, under the conditions of polarization of small platelets (< 0.36  $\mu\text{m}$ ) in an appropriate dielectric matrix (silicon).<sup>22</sup> Thus, the  $\text{LO}_1$  mode should represent the lon-

gitudinal part of the LO-TO splitting of the 1070  $\text{cm}^{-1}$   $\text{TO}_1$  mode.<sup>17</sup> In any case, the contribution of the  $\text{LO}_1$  intensity to the total shoulder intensity  $I_s$

$$I_s = I(\text{LO}_2) + I(\text{TO}_2) + I(\text{LO}_1),$$

is in all cases very small (< 10%).

Figure 1 displays a typical absorption spectrum of an anodically grown silicon oxide ( $C_w=20\%$ ), the thickness being 50 nm. In Fig. 1 we can observe the shoulder of the  $\text{TO}_1$  mode and its deconvolution into three features located at 1144, 1198, and 1250  $\text{cm}^{-1}$ , identified as  $\text{LO}_2$ ,  $\text{TO}_2$ , and  $\text{LO}_1$  modes, respectively, with a full width at half maximum (FWHM) of 68  $\text{cm}^{-1}$ . The  $I_s$  values were measured for the ir spectra of silicon oxides obtained with different  $C_w$ . Figure 2(a) displays the  $I_s/I_m$  ratio, when  $C_w$  increases in the 0–100% range. We can observe a noticeable relative increase in the intensity of the shoulder as  $C_w$  gets higher. The oscillator strength of each of the  $\text{LO}_2$ ,  $\text{TO}_2$ , and  $\text{LO}_1$  modes relative to the  $I_m$  intensity increases as well [Fig. 2(b)]. We have obtained the result that the  $I_s/I_m$  increase is primarily associated with the  $I(\text{LO}_2) + I(\text{TO}_2)$  increase. From XPS measurements we have concluded that this result is related to the increase in disorder in the amorphous silicon oxide films (see below). However, as expected, the  $I(\text{LO}_2)$  relative to the  $I(\text{TO}_2)$  intensity is nearly constant. The values for the thermal and plasma oxides are indicated by arrows in Fig. 2(a); they exhibit the smallest and the highest  $I_s/I_m$  values, respectively.

Figure 3 exhibits a simultaneous increase of the frequencies of the  $\text{TO}_1$  principal mode and the  $\text{LO}_1$ ,  $\text{LO}_2$ , and  $\text{TO}_2$  modes to higher wave number when the water concentration  $C_w$  increases. The positions of the three last modes appear just as sensitive to morphological changes as that corresponding to the  $\text{TO}_1$  mode. This effect is a consequence of the different polarizability of the medium due to the distortion of the silicon oxide network formed in the presence of water. The different chemical environment of the molecular units will split the

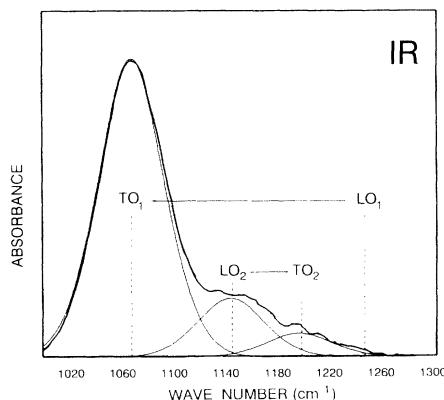


FIG. 1. ir spectrum of the Si-O asymmetric stretching band of the anodic silicon oxide, with a thickness of 50 nm, obtained at room temperature using a current density of 5  $\text{mA cm}^{-2}$ , and its deconvolution in four Gaussian-Lorentzian profiles. The LO-TO splittings are indicated.

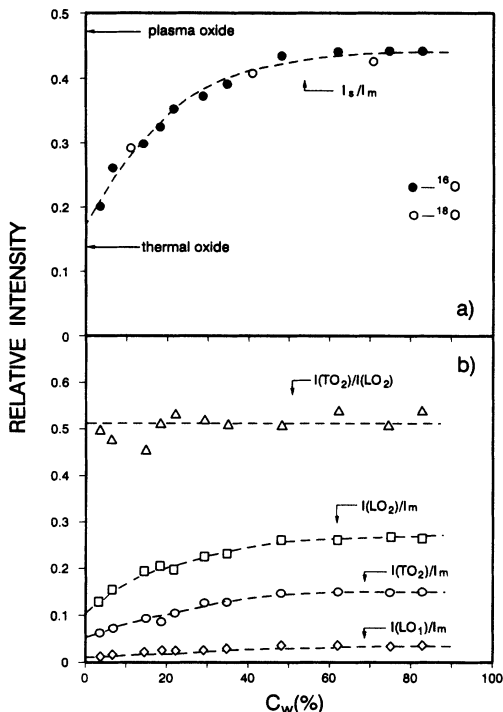


FIG. 2. Variation of the relative intensity between  $I_s$  and  $I_m$  (upper panel), and between  $I(\text{TO}_2)$  and  $I(\text{LO}_2)$ , and of  $I(\text{LO}_2)$ ,  $I(\text{TO}_2)$ , and  $I(\text{LO}_1)$  normalized to  $I_m$  (lower panel), as a function of water concentration.

Si-O band and shift the frequency, resulting in a broad absorption band. Using the  $\text{TO}_1$  frequency as a reference, there is a shift in the position of the  $\text{LO}_2$ ,  $\text{TO}_2$ , and  $\text{LO}_1$  modes from 70 to 78, 127 to 140, and 180 to 184  $\text{cm}^{-1}$ , respectively. These results indicate that the  $\text{LO}_1$ - $\text{TO}_1$  and  $\text{LO}_2$ - $\text{TO}_2$  splitting also increase with water content in the electrolyte.

The disorder-induced effects arising in the presence of water in the electrolyte have also been investigated by XPS measurements. Although the width of the XPS core levels is determined by several contributions (influence of phonons, intrinsic width of the core level, resolution of the spectrophotometer, etc.), we have observed that the

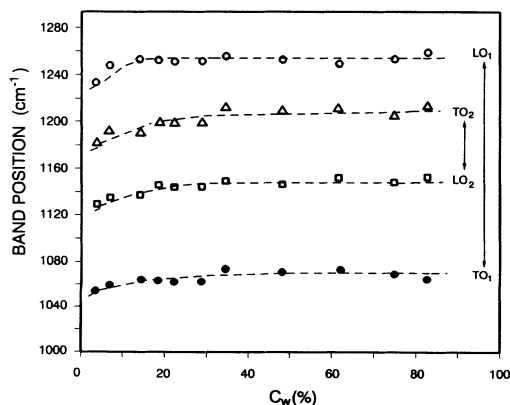


FIG. 3. Plots of the band position as a function of water concentration for the  $\text{LO}_1$ ,  $\text{TO}_1$ ,  $\text{LO}_2$ , and  $\text{TO}_2$  modes.

formation process of the silicon oxide modifies the FWHM values due to a Gaussian homogeneous broadening. Some of the results are shown in Table I. Thermal and plasma oxides show the smallest and the highest FWHM values, respectively. In addition, an increase of the FWHM values is observed in the anodic oxides when  $C_w$  increases.

It is known that XPS is also sensitive to short-range order through induced charge transfer. In fact, the disorder produced in the silicon oxide, in particular the Si-O-Si bridging bond angle and the Si-O bond-length variations due to the distorted network, can influence local orbital hybridization and hence charge transfer.<sup>23,24</sup> Consequently, the resulting distribution of unresolved chemical shifts will give rise to a broadening of the Si 2p and O 1s core levels. Resolution-enhanced XPS studies<sup>23</sup> of the Si 2p levels in thermal oxides have been able to deconvolute three main contributions corresponding to bridging Si-O-Si bond angles associated with four-, six-, and seven- or eight-membered rings, respectively, with the centroid at 144° corresponding to six-membered rings.

Thus, we can conclude that the results for anodic oxides (Table I) are explained either by a broader distribution of bridging bond angles and/or by a relative increase of the frequency of different-from-six-membered rings, compared to the thermal oxide. In the anodic oxides, the presence of OH radicals and  $\text{H}_2\text{O}$  molecules in the network is expected to contribute also to the structural disorder and core-level broadening.

The short-range disorder should affect the valence band (VB) also through the consequent changes in orbital hybridization.<sup>24</sup> The effects expected from theoretical calculations<sup>24</sup> can be observed in the XPS VB density of states shown in Fig. 4. In the curve *a* we observe that the density of states filling the gap at 11 eV between bonding and nonbonding bands has increased. Also, the structure of the bonding bands has smeared out, and the peak at

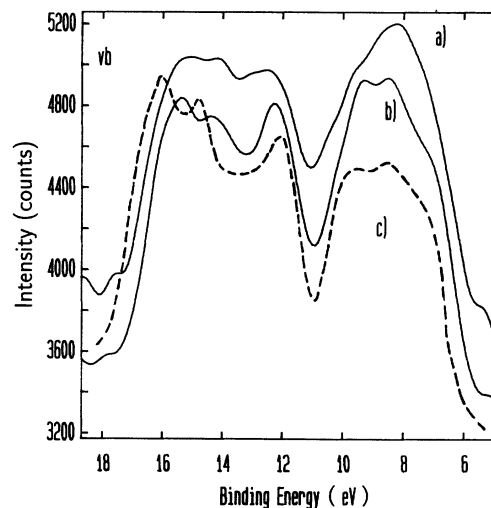


FIG. 4. XPS valence-band spectra for (a) anodic oxide ( $C_w = 100\%$ ), (b) thermal oxide, and (c)  $\alpha$ -quartz (Ref. 28) (crystalline polymorph of  $\text{SiO}_2$ ). The energy reference is the Fermi level of the thermal oxide; the others have been shifted to match the VB edge.

12.5 eV of *p* character with some *s* mixing is hardly distinguishable from the two peaks at higher energy of mainly *s* character. However, the strongest modifications are in the nonbonding band of mainly *p* character at lower binding energies; the structure has also smeared out and the centroid has shifted to lower binding energies.

From these results, it follows that the presence of H<sub>2</sub>O during the oxidation process disrupts the SiO<sub>2</sub> network by forming nonbridging SiOH groups, producing structural changes and disorder in the network. This is also supported by the ir spectra which showed a broad water band at larger wave numbers made up of overlapping H<sub>2</sub>O and OH bands located at 3645 and 3300 cm<sup>-1</sup>, respectively. The amount of water in the sample is indicated by the strength of the broad absorption band in the above region. After thermal treatment under vacuum at 800 °C, this infrared band disappears, i.e., the SiO<sub>2</sub> shows practically no absorption due to hydroxyl groups or absorbed water. On the other hand, a negligible influence of thermal annealing on the relative oscillator strength of the LO<sub>2</sub>-TO<sub>2</sub> pairs is observed. We believed that disorder and large structural defects, created during growth by

clustering of nonbridging groups associated to —OH or H<sub>2</sub>O species, are nearly irreversible and can remain in the network even after loss of the absorbed water by annealing.

To summarize, we have studied the influence of the oxidation conditions on silicon oxide structure, particularly the effect of the concentration of water present during the oxide formation by an electrochemical technique. The work is aimed at exploring the ir asymmetric stretching mode of the Si-O<sub>4</sub> tetrahedra. There is evidence for attributing the different shape of the band to the short-range disorder present in the film. Our analysis provides a quantitative estimate of the longitudinal and transverse optical modes and of the LO-TO splitting. Finally, using the XPS technique we have confirmed the short-range disorder in the anodically grown silicon oxide films through the modifications of the XPS Si 2*p*, O 1*s*, and VB line shapes.

This research work has been supported by the CICYT (MAT92-0258 and MAT92-0093) and by the CAM (CO66/90) of Spain.

- 
- <sup>1</sup>R. Zallen, *The Physics of Amorphous Solids* (Wiley, New York, 1983).
- <sup>2</sup>M. F. Thorpe and F. L. Galeener, *Phys. Rev. B* **20**, 3078 (1980).
- <sup>3</sup>G. Lucovsky, J. Yang, S. S. Chao, J. E. Tyler, and W. Czuba-tyj, *Phys. Rev. B* **28**, 3225 (1983).
- <sup>4</sup>P. Lange, U. Schnakenberg, S. Ullerich, and H. J. Schliwinski, *J. Appl. Phys.* **68**, 3532 (1990).
- <sup>5</sup>F. L. Galeener and G. Lucovsky, *Phys. Rev. Lett.* **37**, 1474 (1976).
- <sup>6</sup>I. W. Boyd and J. I. B. Wilson, *J. Appl. Phys.* **53**, 4166 (1982).
- <sup>7</sup>L. E. Katz, in *VLSI Technology*, edited by S. E. Sze (McGraw-Hill, Singapore, 1983), p. 132.
- <sup>8</sup>P. G. Pai, S. S. Chao, Y. Takagi, and G. Lucovsky, *J. Vac. Sci. Technol. A* **4**, 689 (1986).
- <sup>9</sup>G. Lucovsky, S. Y. Lin, P. D. Richard, S. S. Caho, Y. Takagi, P. Pal, J. E. Keem, and J. E. Tyler, *J. Non-Cryst. Solids* **75**, 429 (1985).
- <sup>10</sup>I. Montero, L. Galán, E. de la Cal, J. Pivin, and J. M. Albella, *Thin Solids Films* **193**, 325 (1990).
- <sup>11</sup>L. Galán, I. Montero, F. Rueda, and J. M. Albella, *Surf. Interface Anal.* **19**, 473 (1992).
- <sup>12</sup>A. Slaoui, E. Fogarassy, C. W. White, and P. Siffert, *Appl. Phys. Lett.* **53**, 1832 (1988).
- <sup>13</sup>A. Slaoui, E. Fogarasy, C. Fuchs, and P. Siffert, *J. Appl. Phys.* **71**, 590 (1992).
- <sup>14</sup>W. Bensch and W. Bergholtz, *Semicond. Sci. Technol.* **75**, 421 (1990).
- <sup>15</sup>D. W. Berreman, *Phys. Rev. B* **130**, 2193 (1963).
- <sup>16</sup>K. B. Koller, W. A. Schmidt, and J. E. Butler, *J. Appl. Phys.* **64**, 4704 (1988).
- <sup>17</sup>C. T. Kirk, *Phys. Rev. B* **38**, 1255 (1988).
- <sup>18</sup>P. Lange, *J. Appl. Phys.* **66**, 201 (1989).
- <sup>19</sup>C. T. Kirk, *Phys. Rev. B* **38**, 1255 (1988).
- <sup>20</sup>P. Grosse, B. Harbeke, B. Heinz, R. Meyer, and M. Offenber, *Appl. Phys. A* **39**, 257 (1986).
- <sup>21</sup>A. Lehmann, L. Schumann, and K. Hübner, *Phys. Status Solidi B* **117**, 689 (1983).
- <sup>22</sup>S. M. Hu, *J. Appl. Phys.* **51**, 5945 (1980).
- <sup>23</sup>F. J. Grunthner and P. J. Grunthner, *Mater. Sci. Rep.* **1**, 85 (1986).
- <sup>24</sup>R. N. Nucho and A. Madhukar, *Phys. Rev. B* **21**, 1576 (1980).